

InP-Based Multiple Quantum Well Structures Grown with Tertiarybutylarsine (TBA) and Tertiarybutylphosphine (TBP): Effects of Growth Interruptions on Structural and Optical Properties

A.L. HOLMES, JR., M.E. HEIMBUCH, G. FISH, L.A. COLDREN, and S.P. DENBAARS

University of California, Santa Barbara, Electrical Engineering Department, Santa Barbara, CA 93016

In this paper, we investigate the effect of interfacial layers on GaInAs(P)/GaInAsP and GaInAs/InP multiple quantum well structures with x-ray diffraction and photoluminescence. We observe a decrease in the room temperature and low temperature photoluminescence intensity as the number of periods is increased which we attribute to the interfaces. Furthermore, different growth interruption schemes show that decomposed As species from TBA have an effect on the structural and optical quality of these structures at both the lower and upper interfaces due to As carry-over. The effect of this carry-over is shown in structural measurements and laser diode results.

Key words: GaInAsP, metalorganic chemical vapor deposition (MOCVD), multiple quantum well (MQW), photoluminescence (PL), tertiarybutylarsine (TBA), tertiarybutylphosphine (TBP), x-ray diffraction (XRD)

INTRODUCTION

Improvements in the performance of 1.3 and 1.55 μm semiconductor lasers has been achieved with the use of quantum well active regions and by the addition of biaxial strain into the quantum wells.^{1,2} Many advanced devices being studied today rely on these high performance active regions to reduce threshold and drive currents,^{3,4} increase modulation bandwidths,⁵ or achieve operational long wavelength vertical cavity devices.⁶ Furthermore, for many applications, short cavities are used. This leads to a smaller active region volume and therefore, more quantum wells being needed to achieve the gain required for lasing. Thus, more interfacial layers exist in the active region which could lead to degradation of the structure's structural and optical characteristics.

This effect of interface degradation has been studied by other authors.⁷⁻¹⁰ In this work, we look at the

effect of this degradation with the use of the liquid organometallic group V sources tertiarybutylphosphine (TBP) and tertiarybutylarsine (TBA) which have been studied because of their lower toxicity and lower chance of catastrophic bubbler failure as compared to arsine and phosphine. In addition, these organometallic sources have a lower decomposition temperature than the conventional sources.¹¹ This effect leads to more active As and P species available to be incorporated into the previously grown layer via diffusion or into the growth of a subsequent layer via column V carry-over. This investigation of interface effects on the properties of InP-based quantum wells is organized as follows. In the next section, the experimental conditions are outlined. Following this, GaInAs(P)/GaInAsP multiple quantum well (MQW) structures grown under standard conditions are studied via x-ray diffraction and photoluminescence. In order to investigate the results presented therein, the standard growth conditions are changed and both GaInAs(P)/GaInAsP and GaInAs/InP MQW struc-

Table I. Partial Pressure for Material Grown in This Study

Material	Strain (%)	TMGa (mTorr)	TMIn (mTorr)	TBA (mTorr)	TBP (mTorr)	Structure Types
GaInAs	0	24.72	29.32	417.34		A,D
Low Strain Quantum Well	≈ 0.6	12.01	29.32	806.8	3303	C
High Strain Quantum Well	≈ 1.3	6.98	29.32	681.6	3303	B
GaInAsP ($\lambda = 1.25 \mu\text{m}$)	0	8.38	29.32	180.13	3303	A,B
Strain Compensated Barrier	≈ -0.5	12.57	29.32	181.53	3303	C
InP	0		29.32		3303	D

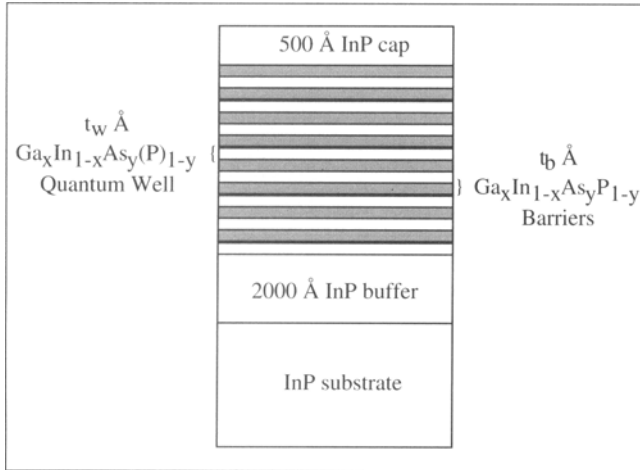
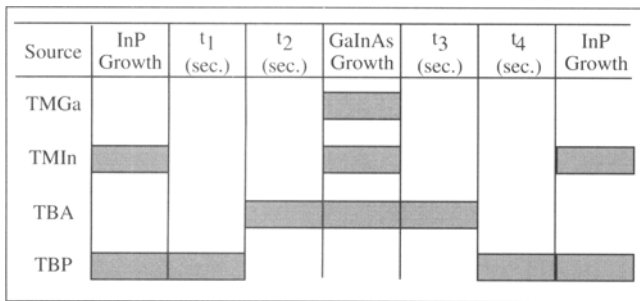
Fig. 1. Schematic cross section of the multiple quantum well structure with N_w quantum wells and N_w+1 barriers used in this study.

Fig. 2. Schematic of growth interruption scheme.

tures are grown and studied.

EXPERIMENTAL CONDITIONS

All samples in this study were grown in a horizontal metalorganic chemical vapor deposition (MOCVD) reactor designed by Thomas Swan. Sn- or Fe-doped (001)InPepi-ready substrates with a 2° misorientation toward the nearest [110] direction were used for all growths. The group III sources used were trimethylindium (TMIn) and trimethylgallium (TMGa) while tertiarbutylarsine (TBA) and tertiarybutylphosphine (TBP) were used as the group V sources. All growths were done at atmospheric pressure and a growth temperature of 645°C as measured by a thermocouple located in the graphite susceptor (uncoated) holding the InP wafer. The run and vent manifolds are pressure balanced and 5.5 slpm of gas flows through the reactor at all times.

Partial pressures used in the samples is summarized in Table I. These partial pressure values were calculated using the source concentration values measured by an ultrasonic cell in the case of the group III sources and the vapor pressure in the case of the group V sources. Normal variations of $\approx 1\%$ around the target value were typically seen for these growths. The general structure schematic used in this study is shown in Fig. 1. Five different types of MQW structures were investigated; these structure are explained in Table I. For type A and B structures, 80\AA wells with were used with 80\AA GaInAsP lattice-matched barriers with a band gap wavelength of $1.25 \mu\text{m}$; for type D structures, 4 ML GaInAs quantum wells were used with 100\AA InP barriers. For type C structures, 95\AA wells were used and the barrier width was varied with the number of periods grown according to:

$$t_b = \frac{N_w}{N_w + 1} \left| \frac{S_w}{S_b} \right| t_w \quad (1)$$

where N_w is the number of quantum wells, S_w is the strain in the well, S_b is the strain in the barrier, and t_w is the well width. Note that in the case above, the strain is not completely compensated after each period; it is only compensated after the last barrier layer has been grown.

These MQW structures were designed to emit light at $1.55 \mu\text{m}$ at room temperature. The structural properties of the MQW structures was measured with a Bede Double Crystal X-ray Diffraction System. For all samples (except type D), the (004) reflection was measured; in some cases, the (115) reflection was also measured to experimentally determine the coherency of the structure to the substrate. The optical properties were measured at both room and low (1.4K) temperature via photoluminescence (PL) except for the type D which are measured only at room temperature. For the type A, B, and C samples, the 488 nm line of the argon laser served as the excitation source. In previous work,¹² we studied the effect of using TBA and TBP on the optical quality of GaInAs/InP quantum wells of varying width. These results showed that, for our reactor, short growth interruptions times (0.5 s) were optimal. The standard growth interruptions sequence is illustrated for an InP barrier and GaInAs quantum well in Fig. 2. This growth interruption scheme has been used in state-of-the art laser diode results¹³⁻¹⁵ and is the nominal growth

interruption scheme used here. In this work, we study the technologically important GaInAs(P)/GaInAsP interfaces. These structures are currently used because strain can be changed within the quantum well without significantly changing the well width. In addition, strain can be added to the barrier with the opposite sign of the barrier to extend the critical thickness of the entire stack by the effect of strain compensation.^{16,17} Increasing the number of quantum wells in the MQW structure systematically allows us to observe the effect of interfaces. Here, we confine ourselves to illustrating and understanding the effect that growth interruptions have on the structural and optical properties of the structure since we are interested in using them for laser diodes.

STRUCTURAL PROPERTIES OF GaInAs(P)/GaInAsP MQW STRUCTURES

Figure 3 shows a (004) x-ray measurement for a 30 period type A structure along with a simulation done using dynamical theory. The zeroth-order peak of the MQW structure is at 0.15% compressive strain. Under the conditions for GaInAs and GaInAsP listed in Table I, the lattice mismatch measured in bulk layers was less than 500 PPM (0.05%). Therefore, we believe that this strain is the effect of the interfaces. The narrow full width at half maximum (FWHM) of the satellite peaks demonstrates the good crystal quality of the structure and no relaxation of the MQW structure. This was confirmed by measuring the (115) reflection of the sample. In order to observe the effect

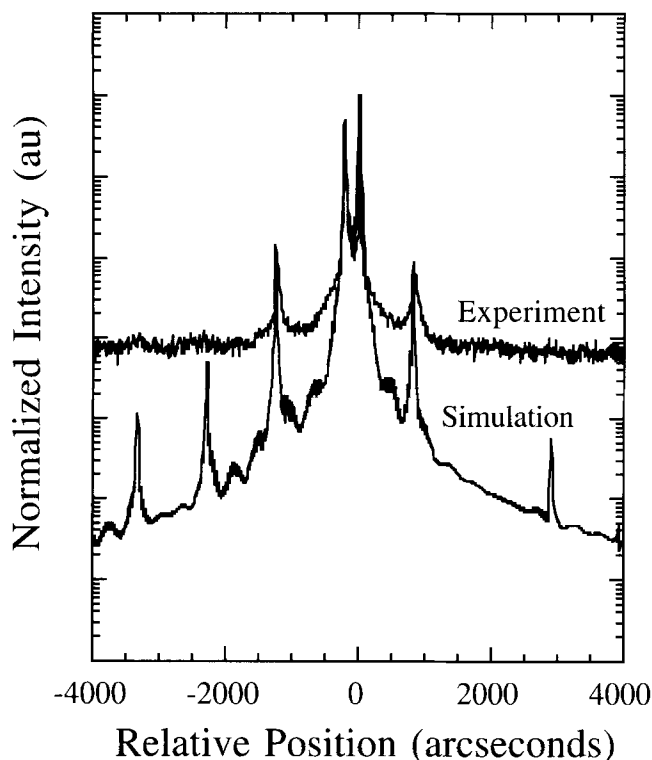


Fig. 3. Normalized x-ray diffraction spectra [(004) reflection] for the 30 period type A sample with corresponding simulation. Note that simulation peaks below the experimental curve cannot be seen because they are below the noise level of our diffractometer.

of the interfaces systematically, type A samples with 6, 10, 20, and 30 periods were measured with a (004) reflection. The x-ray diffraction FWHM was then compared to the simulated results. The results of this calculations are shown in Fig. 4. Note that as the number of periods increases, the FWHM of the x-ray satellite peak for both the experiment and simulation narrows. This is consistent with expectation since, for a periodic structure such as a distributed Bragg reflector (DBR) mirror, the bandwidth (or FWHM here) gets smaller as the number of periods increases. Since there is a deviation from the simulated results, we believe that interfaces formation in the MQW structure is the cause of this deviation. Similar measurements were conducted on the type B and C structures. For the type B, we observed a widening of the x-ray satellite peaks as a function on the number of wells grown; this is consistent with dislocation formation in the structure. This fact was confirmed via a (115) reflection. For the type C structures, the (115) reflection revealed that the MQW structure was coherently strained to the substrate up to 20 periods.

OPTICAL PROPERTIES OF GaInAs(P)/GaInAsP MQW STRUCTURES

The room temperature photoluminescence intensity vs number of periods for the type A and type B structures is shown in Fig. 5. For the type B structure, there is a steep drop in PL intensity above six periods. This drop in intensity is consistent with the previously measured structural properties showing that dislocation formation is leading to decreased optical quality. For the type A structure, a slight decrease in

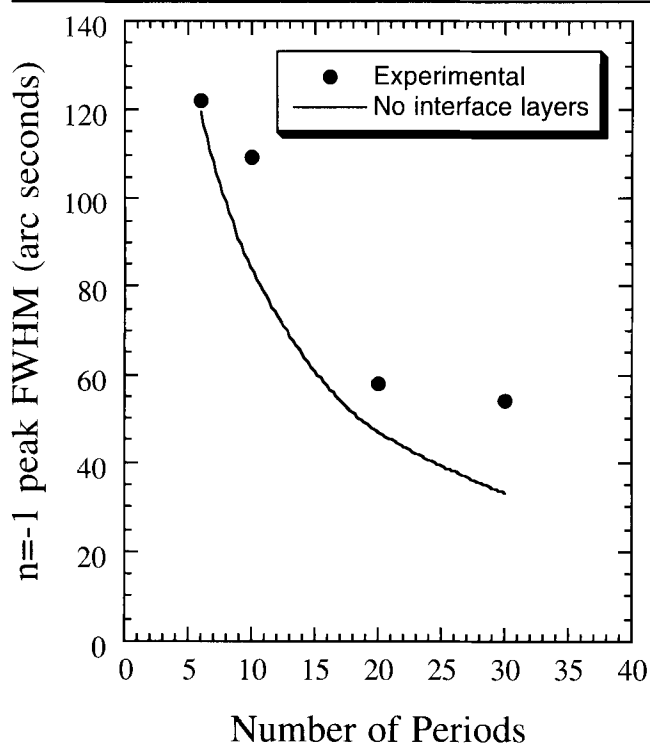


Fig. 4. Comparison of the experimental and theoretical FWHM of the $n = -1$ satellite peaks from x-ray diffraction vs the number of periods.

PL intensity is observed between 20 and 30 periods. Figure 6 shows the FWHM of the low temperature photoluminescence for type A and B structures at room and low temperature. In obtaining this data, two Gaussians were fit to the spectrum and it was assumed that the dominant peak was due to the quantum well luminescence. The type B structure shows a sharp increase in the FWHM at low temperature as more periods are added. The fact that the type A structure does not exhibit this behavior and the structural properties are of high quality, we conclude that this decrease in room temperature PL intensity is not due to dislocations. Since the FWHM at low temperature increases slightly for these structures and also exhibits a broad minima, the most likely cause for this increased broadening is the broadening due to interfacial layers. A FWHM of 8.64 meV was observed which is comparable to that seen with arsine and phosphine. Low temperature photolu-

minescence measurements were also carried out on the type B and C structures. We observed that by using alternating strain in the well and the barrier, the optical properties do not degrade as quickly for the type C structure (strain compensation) as in the uncompensated case (type B). This is attributed to the suppression of dislocation formation in strain compensated structures. However, as is the case with type A, there is a decrease in optical quality with an increase in the number of periods grown in the case of the type C samples.

UNDERSTANDING THE NATURE OF INTERFACE FORMATION WITH TBA AND TBP

The field of interface formation is a very diverse and complex area. In our case, we are interested in understanding the effects of growth interruptions on the structural and optical properties of these MQW structures. In our work discussed in Ref. 12, we believed

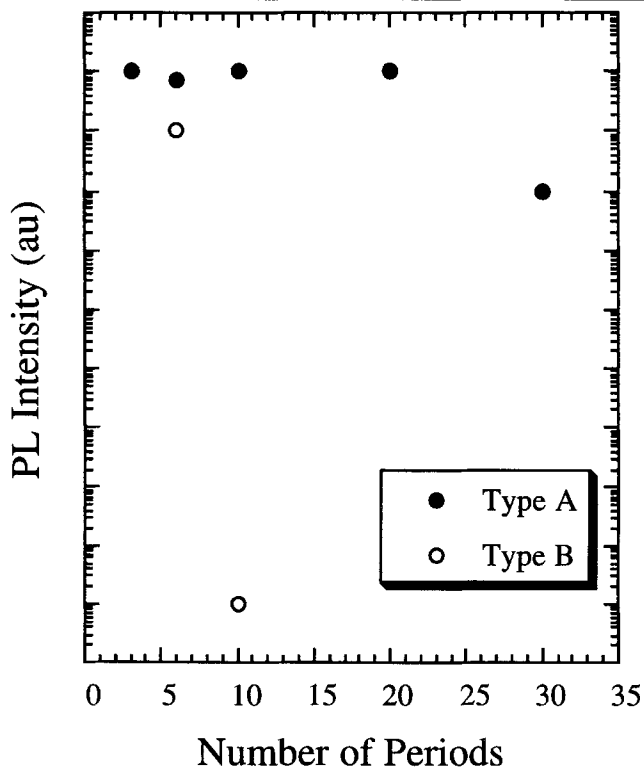


Fig. 5. Integrated intensity of room temperature PL vs the number of periods for type A vs type B samples. The excitation power density used was 10 W/cm^2 .

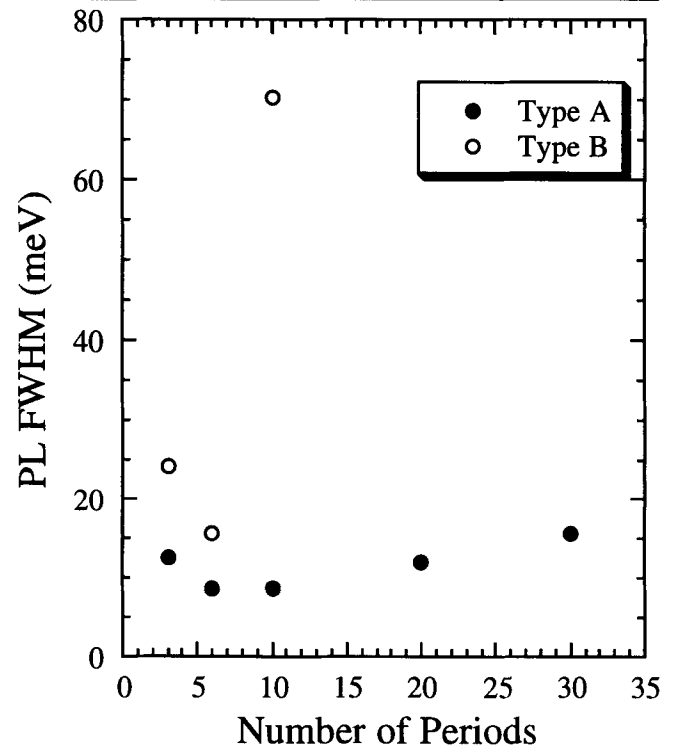


Fig. 6. FWHM of the low temperature PL for the type A and type B structures vs the number of periods. The excitation power density used was 10 W/cm^2 .

Table II. Summary of Growth Interruption Schemes, Structural Results, and Optical Results

Sample	Growth Interruption Scheme		XRD FWHM (arc-s)	Splitting of PL Energy (meV)	PL FWHM (meV)
	t_3 (s)	t_4 (s)			
C-1	0.5: TBA/TBP	0.5: TBA/TBP	67	5.39	10.7
C-2	None	None	86.7	11.06	11.1
C-3	2: H_2 only	0.5: TBA/TBP	72	2.06	7.95
C-4	2.0: TBA/TBP	None	76.1	3.7	8.67
C-5	2.0: TBA/TBP	0.5: TBA/TBP	75	9.83	11.74
C-6	2: H_2 only	0.5: TBA/TBP	60.5	2.08	8.14
C-7	0.5: TBA/TBP	0.5: TBA/TBP	66.1	2.54	7.49

that the use of column V gases during growth interruptions can have two main effects. First, there is *diffusion* of the gaseous column V species into the previously grown layer. This would occur if, at the growth temperature, the column V species desorb from the growth surface. At our growth temperature, this is a well known phenomena. The other effect of a growth interruption is one of *column V carry-over*. In this scenario, the excess column V species left on or over the growth surface is incorporated into the solid when growth of a subsequent layer commences. In order to understand this effect on the GaInAsP/GaInAsP interface, we have grown ten period strain compensated MQW samples with various growth interruptions (type C structures). These samples are summarized in Table II. Based upon the data of others^{18,19} we concentrated on the high-to-low As interface (or well-to-barrier) and have used our standard growth interruptions (0.5 s of TBA and TBP) for the barrier-to-well interface (except in the case of C-2). In the case of these samples, both (004) x-ray diffraction and low temperature PL were measured. Analysis of the PL data involved fitting two Gaussian peaks to the data and assuming the strongest peak is from the MQW emission. As stated elsewhere,²⁰ as long as the InAsP layer is not continuous and longer than the excitonic diameter, discrete lines in the photoluminescence can be seen. This effect was seen in all of the type C samples.

A typical x-ray diffraction curve is shown in Fig. 7 for sample C-6. In our analysis, the $n = -2$ satellite peak was used as a basis of comparison.²¹ From Table II, we note that there are slight changes in the quality

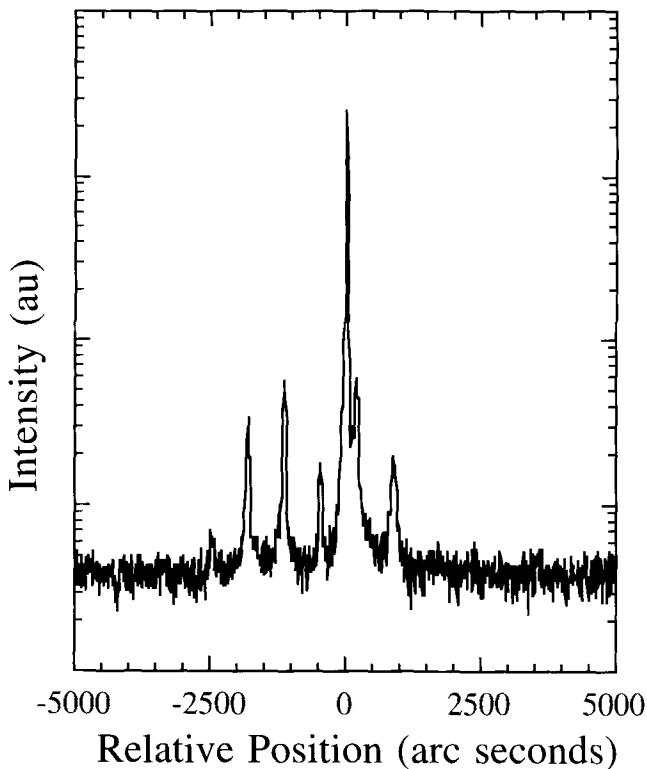


Fig. 7. X-ray diffraction [(004) reflection] for sample C-6.

of the MQW structure when the growth interruptions at the high-to-low As interface are changed. The most drastic changes occur when TBA is left out of the growth interruption scheme. Note that in the case of all of these samples, the changes we are seeing are not dramatic and may only explain some the phenomenon seen in Fig. 5 with relation to the decrease of the MQW's structural and optical quality.

To further probe the effect of growth interruptions, several type D samples (four periods) were grown with varying growth interruption schemes. These structures are summarized in Table III. These structures were only studied via room temperature photoluminescence with an AlGaAs laser diode emit-

Table III. Summary of Growth Interruption Scheme for Type D Samples

Sample	Growth Interruption Scheme			
	t_1 (s)	t_2 (s)	t_3 (s)	t_4 (s)
D-1	0.5: TBP	0.5: TBA	0.5: TBA	0.5: TBP
D-2	0.5: TBP	0.5: H2	0.5: TBA	0.5: TBP
D-3	0.5: TBP	0.5: H2	0.5 H2	0.5: TBP
D-4	1.0: H2	—	0.5: H2	0.5: TBP
D-5	1.5: TBP	0.5: H2	0.5: H2	0.5: TBP
D-6	1.5: TBP	0.5: H2	1.5: TBA	0.5: TBP

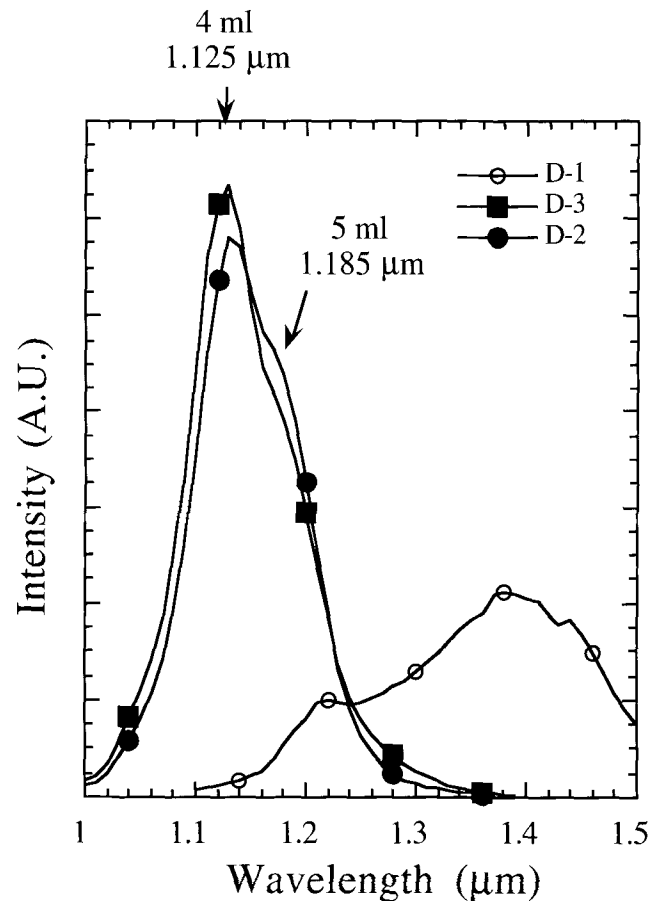


Fig. 8. Effect of changing low-to-high As interface's growth interruption. Note that monolayer splitting is observable at room temperature.

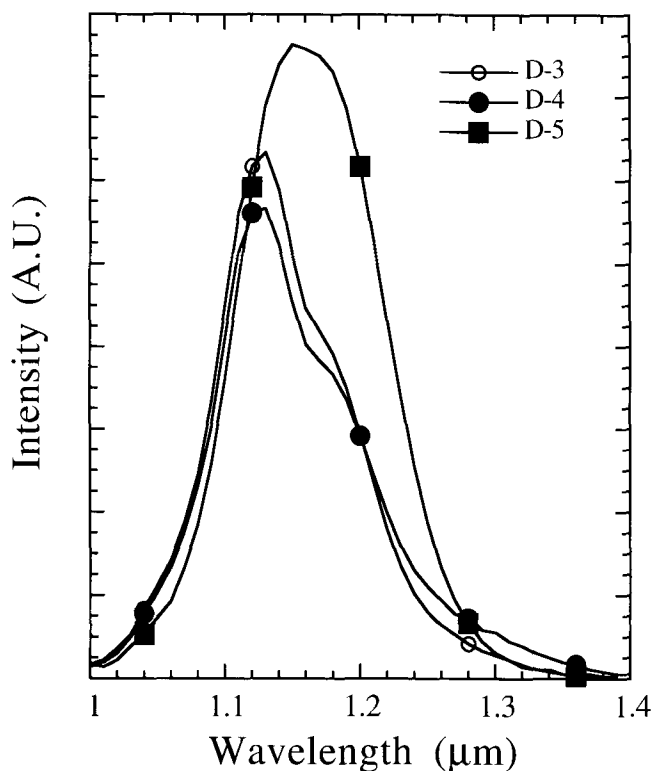


Fig. 9. Effect of diffusion at the lower interface of type D samples.

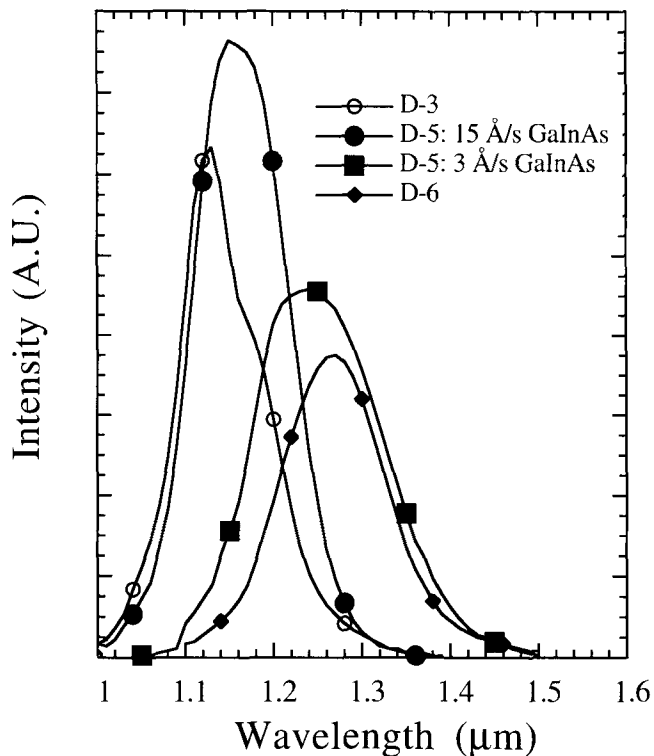


Fig. 10. Effect of carry-over on type D samples.

ting at 789 nm. Figure 8 shows the effect of eliminating TBA from the growth interruptions for the low-to-high As interface (sample D-2) and both interfaces (sample D-3). In this case the effect is dramatic. If TBA is eliminated from the lower interface purge, the PL peak gets to the value expected by theoretical calculations. Also note that eliminating TBA from the

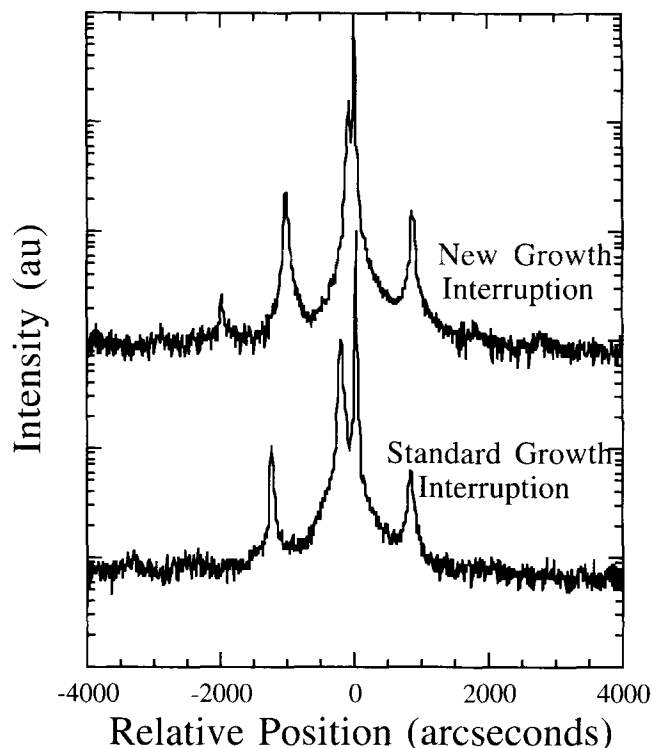


Fig. 11. (004) X-ray diffraction spectra for 30 period type A sample with standard and new growth interruption scheme.

upper interface has a much smaller effect. The effect seen with the D-2 sample is consistent with InAsP forming at the interface.²⁰ Figures 9 and 10 illustrate the effects of diffusion and carry over in the formation of this InAsP layer at the lower interface. In the case of diffusion (Fig. 9), the effect seen is that no drastic changes in PL are seen at up to 1 s interruption times (t_1). At 1.5 s of TBP (sample D-5), degradation of the interface is occurring since the peak has shifted. The reason for the photoluminescence intensity increase in sample D-5 is unknown at this time. We suspect that strain effects due to the interface layer may cause the observed increase. In the case of carry-over (Fig. 10), we see that the introduction of TBA at the upper interface has a very similar effect as decreasing the growth rate in the D-5 samples from 15 to 3 Å/s. In this case, there is more reactive As species at the surface or in the gas phase when growth occurs at a slower rate (i.e., at a higher V/III ratio). For this reason, we believe that it is not diffusion of the column V species that is causing degradation of the interface; instead, we believe that carry-over into the subsequent layer is the dominant effect. Thus, we believe that the elimination of TBA from all growth interruptions leads to a reduction in interface effects for the GaInAs/InP interface. For GaInAs(P)/GaInAsP interfaces, we believe that the elimination of both column V species from both sides of the quantum well (the high As-containing layer). This improvement in both cases is due to reduced As adsorption at the growth surface in low column V over-pressure conditions.²²

To confirm the improvement in the MQW structure, the 30 period type A structure was regrown

under the same conditions with the new growth interruption scheme. The results of the (004) x-ray diffraction measurements are shown in Fig. 11. Note that the improvement observed is due to a reduction in the effect of the interfaces of the structure. This effect further illustrated itself in laser diode results. Broad-area laser diodes were fabricated with four unstrained GaInAs quantum well active regions. The device structure and processing has been discussed elsewhere.¹² When TBA was used in the growth interruptions, the threshold current density was 740 A/cm² for a 50 × 500 μm² device; when TBA was eliminated from the growth interruptions, the threshold current density jumped to 1200 A/cm² for the same device dimensions. Since the interface effect has been reduced, the strain induced by them in the active region is also reduced; this leads to the observed threshold density increase.

CONCLUSIONS

In this paper, InP-based MQW structures are studied using TBA and TBP. The results show that the standard interruption scheme that was used for a low number of wells is not the optimized interruption scheme as more wells are added. Our data shows that the use of TBA in the growth purge leads to decreased optical and structural properties via carry-over into the subsequent growth layer. We further show that short growth interruption times with H₂ only leads to the most optimized structural and optical properties. The improvement of the MQW structure was experimentally shown in both MQW structures and laser diode results.

REFERENCES

1. A. Mathur, J.S. Osinski, P. Grodzinski and P.D. Dapkus, *IEEE Photonics Technol. Lett.* 5, 753 (1993).
2. P.J.A. Thijs, J.J. M. Binsma, L.F. Tiemeijer and T. van Dongen, *IOOC-ECOC '91*. 17th European Conf. Optical Communication ECOC '91. 8th Intl. Conf. Integrated Optics and Optical Fibre Communication IOOC '91 (1991), p. 31.

3. J.S. Osinski, Y. Zou, P. Grodzinski, A. Mathur and P.D. Dapkus, *IEEE Photonics Technol. Lett.* 4, 10 (1992).
4. S. Ae, T. Terakado, T. Nakamura, T. Torikai and T. Uji, *J. Cryst. Growth* 145, 852 (1994).
5. P.A. Morton, R.A. Logan, T. Tanbun-Ek, P.F. Sciortino Jr., A.M. Sergent, R.K. Montgomery and B.T. Lee, *Elect. Lett.* 28, 2156 (1992).
6. D.I. Babic, J.J. Dudley, K. Streubel, R.P. Mirin, J.E. Bowers and E.L. Hu, *Appl. Phys. Lett.* 66, 1030 (1995).
7. K. Streubel, F. Scholz, V. Harle, M. Bode, M. Grundmann, J. Christen and D. Bimberg, *Third Intl. Conf. Indium Phosphide and Related Mater.* Cat. No.91CH2950-4 (1991), p. 468.
8. G. Landgren, P. Ojala and O. Ekstrom, *J. Cryst. Growth* 107, 573 (1991).
9. J. Hergeth, D. Grutzmacher, F. Reinhardt and P. Balk, *J. Cryst. Growth* 107, 537 (1991).
10. C.A. Tran, J.T. Graham, J.L. Brebner and R.A. Masut, *J. Electron. Mater.* 23, 1291 (1994).
11. S.H. Li, C.A. Larsen, N.I. Buchan and G.B. Stringfellow, *J. Electron. Mater.* 18, 457 (1989).
12. M.E. Heimbuch, A.L. Holmes Jr., C.M. Reaves, M.P. Mack, S.P. DenBaars and L.A. Coldren, *J. Electron. Mater.* 23, 87 (1994).
13. M.E. Heimbuch, A.L. Holmes Jr., M.P. Mack, S.P. DenBaars, L.A. Coldren and J.E. Bowers, *Elect. Lett.* 29, 340 (1993).
14. V. Jayaraman, M.E. Heimbuch, L.A. Coldren and S.P. DenBaars, *Elect. Lett.* 30, 1492 (1994).
15. R. Yu, R. Nagarajan, T. Reynolds, A.L. Holmes, J.E. Bowers, S.P. DenBaars and C.-E. Zah, *Appl. Phys. Lett.* 65, 528 (1994).
16. T. Tsuchiya, M. Komori, R. Tsuneta and H. Kakibayashi, *J. Cryst. Growth* 145, 371 (1994).
17. B.I. Miller, U. Koren, M.G. Young and M.D. Chien, *Appl. Phys. Lett.* 58, 1952 (1991).
18. R. Meyer, M. Hollfelder, H. Hardtdegen, B. Lengeler and H. Luth, *J. Cryst. Growth* 124, 583 (1992).
19. A.G. Norman, B.R. Butler, G.R. Booker and E.J. Thrush, *Microscopy of Semiconducting Materials 1989*. Proc. Royal Microscopical Soc. Conf. (1989), p. 311.
20. J. Bohrer, A. Krost and D. Bimberg, *Appl. Phys. Lett.* 60, 2258 (1992).
21. T.H. Chiu, J.E. Cunningham, T.K. Woodward and T. Sizer II, *Appl. Phys. Lett.* 62, 340 (1993).
22. W. Seifert, X. Liu and L. Samuelson, *Semiconductor Heterostructures for Photonic and Electronic Applications Symp.* 97 (1993).